⌘ *Author's Choice*

THE JOURNAL OF BIOLOGICAL CHEMISTRY VOL. 286, NO. 7, pp. 5813–5822, February 18, 2011

Folding, Quality Control, and Secretion of Pancreatic Ribonuclease in Live Cells*[S]

Received for publication, August 3, 2010, and in revised form, December 2, 2010 Published, JBC Papers in Press, December 14, 2010, DOI 10.1074/jbc.M110.171694

Roger Geiger, Matthias Gautschi, Friederike Thor, Arnold Hayer, and Ari Helenius[1]

From the Institute of Biochemistry, ETH Zürich, 8093 Zürich, Switzerland

Although bovine pancreatic RNase is one of the best characterized proteins in respect to structure and *in vitro* refolding, little is known about its synthesis and maturation in the endoplasmic reticulum (ER) of live cells. We expressed the RNase in live cells and analyzed its folding, quality control, and secretion using pulse-chase analysis and other cell biological techniques. In contrast to the slow *in vitro* refolding, the protein folded almost instantly after translation and translocation into the ER lumen ($t_{½} < 3$ min). Despite high stability of the native protein, only about half of the RNase reached a secretion competent, monomeric form and was rapidly transported from the rough ER via the Golgi complex ($t_{½} = 16$ min) to the extracellular space ($t_{½} = 35$ min). The rest remained in the ER mainly in the form of dimers and was slowly degraded. The dimers were most likely formed by C-terminal domain swapping since mutation of Asn^{113}, a residue that stabilizes such dimers, to Ser increased the efficiency of secretion from 59 to 75%. Consistent with stringent ER quality control *in vivo*, the secreted RNase in the bovine pancreas was mainly monomeric, whereas the enzyme present in the cells also contained 20% dimers. These results suggest that the efficiency of secretion is not only determined by the stability of the native protein but by multiple factors including the stability of secretion-incompetent side products of folding. The presence of *N*-glycans had little effect on the folding and secretion process.

Our current understanding of protein folding is mainly derived form *in vitro* studies in which proteins are denatured and then allowed to refold. A spectrum of powerful methods exists to monitor the refolding process, and an impressive body of detailed information is available on the refolding of many proteins. However, because the conditions typically used during the refolding experiments are far removed from those prevailing in the cytosol of cells or in the lumen of the endoplasmic reticulum (ER),[2] it is not clear to what degree the results are applicable to *in vivo* maturation of proteins. Differences exist in respect to temperature, pH, ionic milieu, crowding, etc. *In vitro* refolding is generally performed in the absence of folding enzymes, chaperones, and other interacting factors. Moreover, whereas folding in live cells can be cotranslational and therefore vectorial, refolding involves by definition the complete polypeptide chain.

The substrate proteins used for *in vitro* refolding studies are generally small, monomeric, soluble, and devoid of covalent post-translational modifications. The larger and more complex a protein, the lower tends to be the refolding efficiency. In contrast, proteins whose folding has been analyzed in live cells are often large and complex multidomain proteins such as influenza HA (1), tyrosinase (2), and the cystic fibrosis transmembrane conductance regulator (3). These begin folding as growing nascent chains and reach their native conformation post-translationally several minutes or even hours after translation. They interact with numerous chaperones, and many undergo oligomeric assembly before they are exported out of the ER.

Most of the work that has been performed so far to analyze folding *in vivo* has focused on oxidative folding in the ER because it is possible to rapidly interrupt the folding process by addition of membrane-permeable alkylating agents to block further disulfide formation (1). In favorable cases, this allows identification and characterization of intermediates in the oxidative folding process. The association of nascent chains and newly synthesized proteins with chaperones, folding sensors, degradation machinery, and lectins is generally detected using immunoprecipitation. Additional information is obtained using perturbations in the form of inhibitors, mutant proteins, and genetic manipulation of the cell.

The type of information gained from *in vivo* studies is not easily correlated with the detailed information acquired using *in vitro* refolding and biophysical read-outs. Therefore, in this study, we try to bridge between the two approaches by analyzing the *in vivo* folding and maturation of one of the best studied *in vitro* refolding substrates, bovine pancreatic RNase. It is the protein used in Anfinsen's pioneering refolding studies (4), and its refolding continues to be the subject of detailed analysis (5, 6). It is a monomeric, stable, soluble, secretory enzyme composed of 124 amino acids (6). Two disulfide bonds link together surface loops, and two others connect one of the α-helices to a β-sheet. The disulfides contribute to the high stability (7). Bovine RNase has one consensus sequence for *N*-linked glycosylation (Asn^{34}) and occurs in a nonglycosylated (RNase A) and a glycosylated form (RNase B).

MATERIALS AND METHODS

Materials—Cell culture reagents were from Invitrogen and Sigma; purified bovine RNase A and B, protein A-Sepharose

* This work was supported by the Swiss National Research Foundation and ETH Zurich.

[S] The on-line version of this article (available at http://www.jbc.org) contains supplemental Fig. 1.

⌘ *Author's Choice*—Final version full access.

[1] To whom correspondence should be addressed: Schafmattstrasse 18, 8093 Zürich, Switzerland. Tel.: 41-44-632-68-17; Fax: 41-44-632-12-69; E-mail: ari.helenius@bc.biol.ethz.ch.

[2] The abbreviations used are: ER, endoplasmic reticulum; Endo H, endoglucosidase H; IP, immunoprecipitation.

CL-4B beads, DTT, tunicamycin, brefeldin A, aprotinin, pepstatin, leupeptin, and chymostatin from Sigma. *N*-Ethylmaleimide was from Fluka; CHAPS was from Pierce; restriction enzymes and endoglucosidase H (Endo H) were from New England Biolabs, and TurboPfu® DNA polymerase from Stratagene. Monoclonal HA.11 antibody was from Covance, rabbit polyclonal affinity purified bovine RNase antibody from Abcam. The calnexin and mannosidase II antibodies have been described in Refs. 8, 9. The Sec13 antibody was a kind gift from Y. Misumi (10). Alexa Fluor secondary antibodies were purchased from Molecular Probes (Invitrogen), anti-rabbit IgG HRP, ECL Plus Western blotting detection system, and Promix [^{35}S]methionine/cysteine were from GE Healthcare, and Superfect® Transfection Reagent was from Qiagen. All chromatographic experiments were performed on an Amersham Biosciences Aekta purifier system. Superdex 75 HR 10/30 column was from Pharmacia.

Plasmid Construction—The bovine RNase constructs contained the first 24 residues from influenza HA, *i.e.* HA signal sequence and HA tag followed by the synthetic mature sequence of bovine RNase (11), in the vector pSVSPORT1 (Invitrogen), as described for human RNase (12). Point mutations were introduced by single base pair exchange using the QuikChange® site-directed mutagenesis protocol (Stratagene). All sequences were checked by sequencing.

Cell Culture, Transfection, Labeling, and Immunoprecipitation (IP)—CHO cells were maintained in minimal essential medium α supplemented with 10% fetal calf serum. CHO cells were transiently transfected using Superfect according to the manufacturer's instructions (Qiagen). Metabolic labeling (pulse-chase) and IP were performed as described (13). Various drugs were added to cells during the pulse and the chase with the following final concentrations: DTT (5 mM), brefeldin A (5 mg/ml), tunicamycin (5 mg/ml), and castanospermine (1 mM).

Enzyme Treatments—After boiling of samples in SDS and DTT, Endo H was added, and the mixture was incubated for 1 h at 37 °C. Trypsin digestion was performed as follows; after IP, immunocomplexes derived from cells and medium were resuspended in 20 μl Hepes buffered saline (HBS) and subjected to trypsin digestion (10 mg/ml trypsin for 5 min at 20 °C).

SDS-PAGE—Samples were analyzed by 15% SDS-PAGE. Gels were visualized by a Storm 860 PhosphorImager (Molecular Dynamics) and quantified using ImageJ software.

Indirect Immunofluorescence—CHO cells grown on 12-mm coverslips were transfected, fixed, and stained as described (14). Confocal fluorescence microscopy was performed using a Zeiss LSM 510 Meta system. For wide field fluorescence microscopy, an Olympus IX71 microscope was used.

Image Analysis—CellProfiler (15) routines were used for semiautomated analysis of epifluorescence images. After background subtraction, Golgi outlines were detected based on mannosidase II staining and cellular outlines based on RNase signals. The ratio of RNase fluorescence in Golgi/total was determined for each cell. $n \geq 200$ cells were analyzed per condition.

Preparation of Domain Swapped Bovine RNase Dimers—Oligomers were obtained as described (16).

Gel Filtration—A Superdex 75 HR 10/30 column was equilibrated and run at 0.5 ml/min in HBS buffer. Fractions of 0.5 ml were collected for further analysis.

Cell Fractionation—CHO cells were washed with PBS and homogenization buffer (HB; 250 mM sucrose, 10 mM Hepes, pH 7.4, 1 mM EDTA). After pelleting, the cells were resuspended in HB containing protease inhibitors and disrupted by 20 passages through a 25-gauge needle. Nuclei and unbroken cells were spun down at 1100 $\times$ *g*. The supernatant was centrifuged in a Beckmann TLA 120.2 rotor at 100,000 $\times$ *g* for 60 min. The microsomes were resuspended by loose douncing in 0.5 ml of HB and loaded on top of linear 0–15% iodixanol gradients followed by centrifugation in a Beckmann SW41 rotor at 25,000 rpm for 18 h. 12 fractions were collected.

Preparation of Bovine Pancreatic Tissue and Juice—Fresh bovine pancreas was obtained from the slaughterhouse. To isolate pancreatic juice, the end of the pancreas was cut out. The juice was carefully removed from the duct with a pipette and then cleared by centrifugation. Pancreatic tissue (1.5 g) was cut up into small pieces and homogenized in the cold in 2 ml of buffer (HBS, pH 7.4, 1 mM PMSF, 2% CHAPS, protease inhibitors). The suspension was cleared by centrifugation, and the supernatant was collected.

RESULTS

Synthesis and Glycosylation—CHO cells were transfected with bovine RNase constructs. To ensure constant and efficient signal sequence cleavage in these cells, we used a construct with the signal sequence of influenza HA followed by a HA tag. Folding and secretion of the RNase was analyzed using a pulse-chase approach with short (1–4 min) pulses of [^{35}S]methionine and [^{35}S]cysteine. Immediately after the pulse, or after chase periods of variable length in the presence of unlabeled amino acids, *N*-ethylmaleimide containing stop buffer was added to block further protein synthesis and to inhibit post-lysis folding by alkylating remaining free sulfhydryl groups (1). The cells were lysed with CHAPS in the presence of *N*-ethylmaleimide and protease inhibitors, and medium and lysate immunoprecipitated with polyclonal antibodies that recognized both native and denatured RNase molecules. The precipitates were reduced and subjected to SDS-PAGE followed by autoradiography.

Two bands of approximately equal intensity were observed, the faster migrating with a molecular mass of 13–14 kDa and the slower with 15–16 kDa (Fig. 1, *lanes 1* and *5*). When the cells were treated with the glycosylation inhibitor tunicamycin, only the faster migrating band was present indicating that it corresponded to the unglycosylated form RNase A, and the slower band to the glycosylated form RNase B (Fig. 1, *lanes 4* and *8*). Thus, glycosylation of the RNase in CHO cells was limited to about half of the molecules.

Even when exit of the RNase from the ER to the Golgi complex was blocked using brefeldin A, no further glycosylation occurred over time (Fig. 1, *lanes 3* and *7*). This suggested that glycosylation of the RNase was co-translational and that folding occurred rapidly. It is noteworthy that when DTT, a membrane-permeable reducing agent, was added to prevent oxidative folding (17), the fraction of glycosylated bovine

RNase continued to increase during the chase with virtually full conversion to RNase B within 60 min (Fig. 1, *lanes 2* and *6*). Such post-translational addition of *N*-glycans was consistent with results obtained for some other glycoproteins indicating that glycosylation can occur post-translationally if a protein remains incompletely folded (18, 19).

Folding—To determine the rate of folding, we took advantage of the conversion of RNase from a protease-sensitive to a protease-resistant form (11, 20). The RNase secreted into the medium was fully resistant to trypsin as shown in (Fig. 2*A*). Less than 10% of the labeled protein was resistant at the end of a 1-min pulse (Fig. 2*B*). However, after a 4-min pulse 80%, and after a further 4 min of chase, 95% of the labeled protein was resistant. This indicated that bovine RNase folded to a trypsin-resistant form with a half time of less than 3 min after completed synthesis.

To determine how rapidly the folding yielded a transport-competent protein, we took advantage of the difference in DTT sensitivity of incompletely folded and fully folded proteins by performing a wash-out/readdition experiment (21). DTT rapidly reduces disulfide bonds in misfolded and incompletely folded proteins but generally does not reduce disulfides in folded proteins (17). Therefore, it prevents exit of proteins that are not yet fully folded from the ER but does not affect secretion of proteins that have reached the folded form (22).

After inclusion in the pulse medium to prevent folding of the newly synthesized RNase, DTT was washed away during the chase for a time window ranging from 1 to 15 min (Fig. 2, *D* and *E*). During this DTT-free period, oxidation and folding could take place. When the reducing agent was added again, further oxidative folding was stopped, and any proteins still incompletely folded were reduced. Those RNase molecules that had managed to reach the fully folded form remained unaffected and were secreted. After readdition of DTT, the cells were chased for a further 60 min to allow quantitative secretion of such molecules.

Consistent with rapid folding, a window of 1 min without DTT was enough to allow 25% of the newly synthesized RNase molecules to reach a DTT-resistant and transport-competent form (Fig. 2*E*). The half-time was 2.1 min, and af-

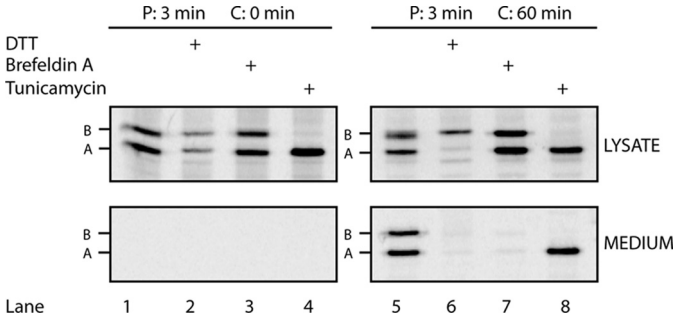

FIGURE 1. **Bovine RNase A (*A*) and B (*B*) are secreted in CHO cells.** Cells transiently expressing bovine RNase were pulsed for 3 min (*P*, 3 min) (0.2 mCi/ml [^{35}S]Met/Cys) and either directly treated with stop buffer (*C*, 0 min) or after 1-h chase (*C*, 60 min). After IP of RNase from cell lysates or medium, samples were subjected to reducing SDS-PAGE followed by autoradiography. Where indicated, drugs were added to the pulse and chase media.

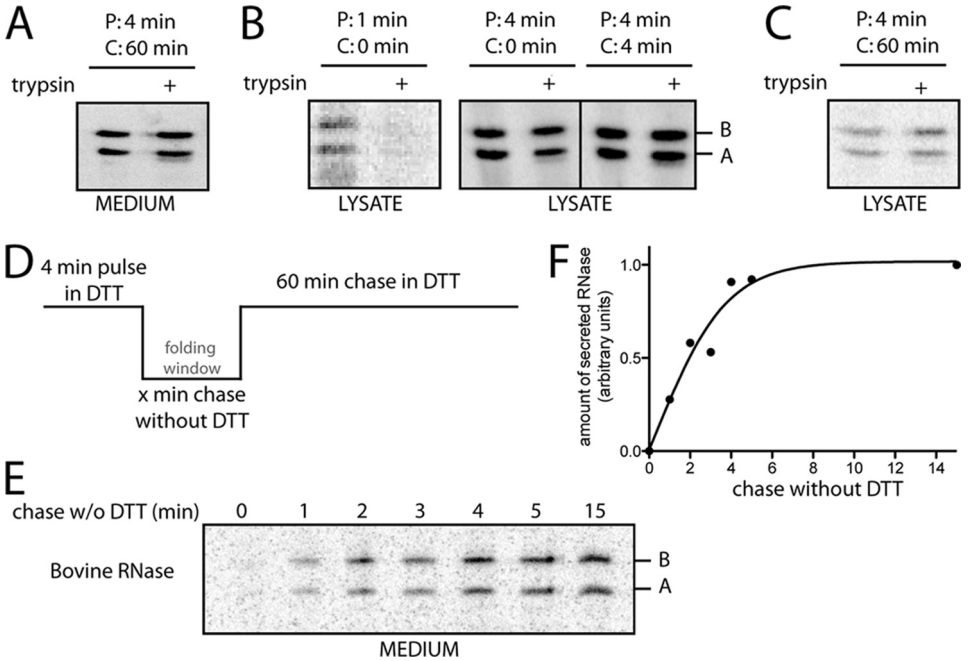

FIGURE 2. **Folding of bovine RNase occurs rapidly in the ER of CHO cells.** Cells expressing bovine RNase were pulse-labeled (0.5 mCi/ml [^{35}S]Met/Cys) with or without chase (times are indicated). Folding was assayed by trypsin resistance of RNase. After IP of RNase molecules with RNase antibody from the media (*A*) or cell lysates (*B* and *C*), samples were subjected to trypsin digestion for 5 min at 20 °C followed by reducing SDS-PAGE and autoradiography. *D* and *E*, pulse-chase (0.5 mCi/ml [^{35}S]Met/Cys) of bovine RNase in CHO cells to determine folding after DTT washout and readdition. Cells were labeled in the presence of DTT (4 min) and subsequently chased in medium lacking DTT for the time indicated (chase without DTT), followed by a chase for 60 min in medium supplemented with DTT. After IP of secreted RNase with RNase antibody from the medium, samples were subjected to reducing SDS-PAGE followed by autoradiography. *F*, quantification of secreted RNase molecules. The amount of secreted RNase after 15 min of folding time in the absence of DTT was set to 1. The other data points were normalized to it and fitted with a Boltzmann sigmoidal curve. A half-time of 2.1 min was calculated. *A*, RNase A; *B*, RNase B.

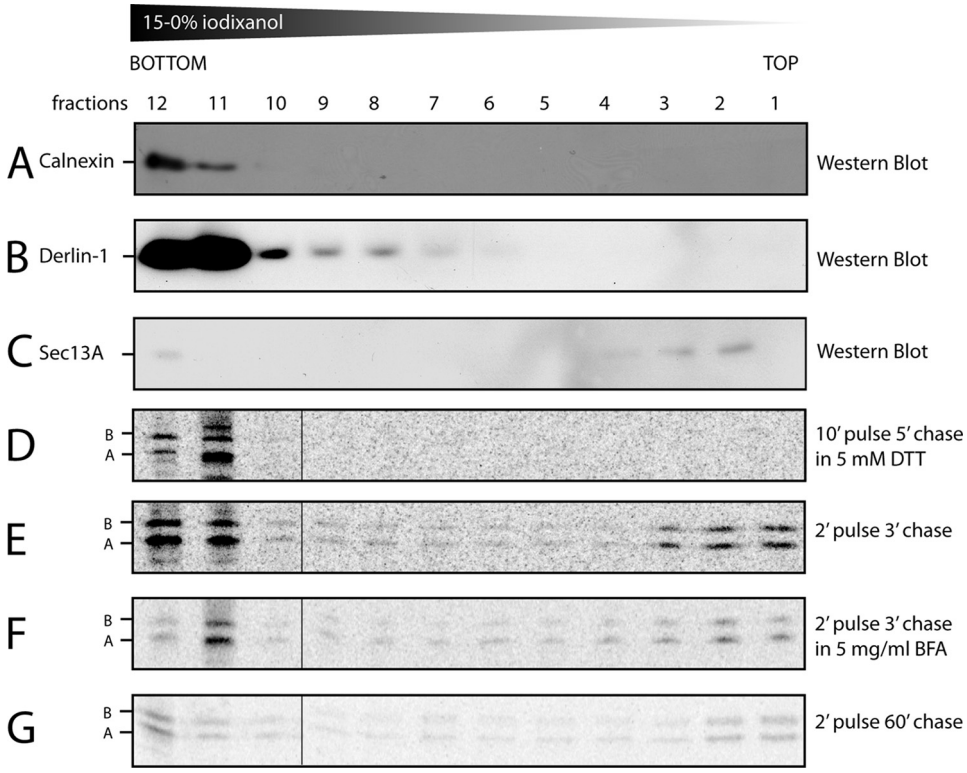

FIGURE 3. **Movement of newly synthesized bovine RNase from dense to light microsomal fractions.** Microsomal vesicles were prepared from CHO cells and separated on linear 0–15% iodixanol gradients. Gradient fractions were TCA precipitated and immunoblotted with calnexin (*A*), derlin-1 (*B*), and Sec13 (*C*) antibodies. *D–G*, CHO cells were pulse-labeled (0.5 mCi/ml [^{35}S]Met/Cys) and chased for the indicated times. Where indicated, drugs were added to the starvation, pulse, and chase media. Cells were homogenized, and microsomal vesicles were loaded on the gradients. After centrifugation, fractions were collected from the top and immunoprecipitated with RNase antibodies followed by reducing SDS-PAGE and autoradiography. *A*, RNase A; *B*, RNase B.

ter 4 min, the maximum level of secretion competence had already been reached (Fig. 2*F*).

Thus, the results indicated that the rate of folding of newly synthesized bovine RNase A and B in the cell was orders of magnitude faster than that observed for the RNase during *in vitro* refolding, a process that can take several hours (4, 23). The folding time was also unusually short compared with most other proteins that have been analyzed in the ER of live cells (24). No difference in the rate was observed between the glycosylated and nonglycosylated forms. Also, there seemed to be little difference whether folding was allowed to occur normally or "jump started" post-translationally by DTT washout. The normal *in vivo* oxidative folding is, in fact, likely to occur post-translationally as well, because in each of the native disulfides at least one of the cysteines is still located within the ribosome or translocon complex at the time of chain termination. Attempts to demonstrate association with BiP and calnexin failed (data not shown) suggesting that if interactions with these chaperones occurred, they were brief.

Export from Rough ER—Protein synthesis and translocation of newly synthesized proteins occurs in the rough ER. To monitor the movement of newly synthesized RNase from the rough to the smooth ER (where the ER exit sites are located) and to the ER-Golgi intermediate compartment, we took advantage of the buoyant density difference between vesicles derived from rough and smooth membrane domains. Optimal separation by isopycnic density gradient centrifugation was achieved when microsomal vesicle fractions from CHO cells were subjected to ultracentrifugation in 0–15% linear iodixanol gradients. Immunoblotting of gradient fractions showed that calnexin (an abundant ER chaperone) and derlin-1 (a component of the ER-associated degradation machinery) were present in a dense vesicle fraction, whereas Sec13A (a component of the COP II coat of ER exit sites, and thus part of the smooth ER) was found mainly in light vesicles (Fig. 3, *A–C*).

To analyze the distribution of newly synthesized bovine RNase, RNase-expressing cells were first pulse-labeled and chased in the presence of DTT to prevent folding and export. IP showed that the labeled bovine RNase was only present in dense vesicles (Fig. 3*D*). Thus, when oxidative folding was prevented, the RNase was retained in the rough ER.

When cells were pulsed for 2 min and chased for 3 min in the absence of DTT, we observed 30% of the labeled RNase in top fractions (Fig. 3*E*). Although the rapidity of the transfer made it hard to define a clear time course, this suggested that already shortly after translation a fraction of the RNase moved from the rough to the smooth ER. After a prolonged chase (60 min) to allow the secretion-competent RNase to drain out of the ER and leave the cell, the distribution of remaining labeled RNase was 70% in dense and 30% in light vesicles (Fig. 3*G*). The transport-incompetent RNase molecules retained in the ER at this late time were thus distributed between the rough and smooth elements of the ER. Similar amounts of RNase (30%) were found in the top fractions, when cells were pulsed

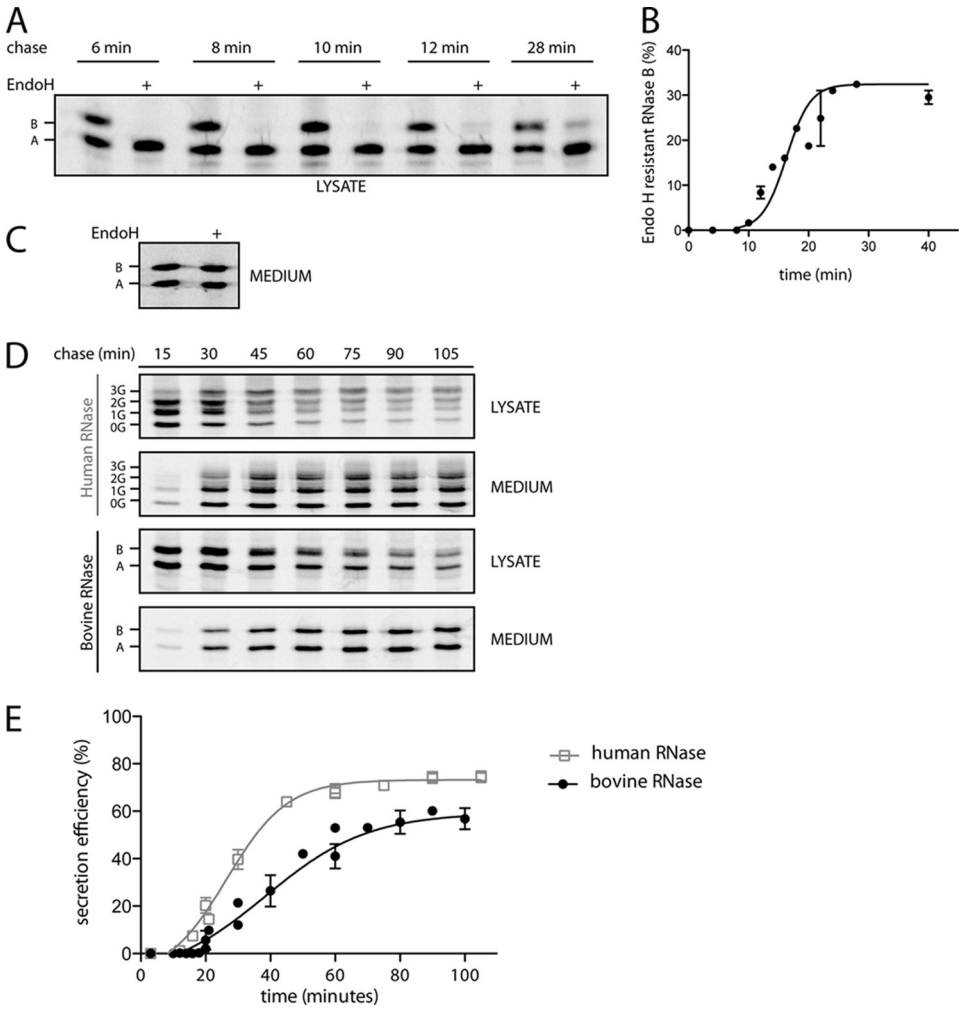

FIGURE 4. **Bovine and human RNase are secreted rapidly but with different efficiency.** *A*, CHO cells expressing bovine RNase were pulse-labeled (0.5 mCi/ml [^{35}S]Met/Cys) for 2 min and chased for the indicated times. After IP of RNase from cell lysates or media with RNase antibody, samples were subjected to Endo H digestion followed by separation on reducing SDS-PAGE and autoradiography. *B*, the percentage of Endo H-resistant RNase B was plotted *versus* chase time and was fitted with a Boltzmann sigmoidal curve. A half-time of 16 min was calculated. *Error bars* represent the S.E. *C*, secreted RNase after a 60-min chase was used as a control. *D*, one representative example of three independent pulse-chase experiments of human and bovine RNase in CHO cells. After IP of RNase from cell lysate or medium, samples were subjected to reducing SDS-PAGE followed by autoradiography (quantification by ImageJ). *E*, the fraction of secreted RNase of total RNase (cells and medium) was plotted *versus* chase time. Data points represent means ± S.E. and were fitted with a Boltzmann sigmoidal curve. *A*, RNase A; *B*, RNase B.

and chased in the presence of brefeldin A to prevent export beyond the ER-Golgi intermediate compartment (Fig. 3*F*).

Taken together, the cell fractionation results suggested that the RNase begun to leave the rough ER immediately when oxidative folding was completed and that movement beyond the ER-Golgi intermediate compartment occurred after 5 min or longer. The transport-incompetent RNase that remained in the ER after 60 min was mainly retained in the dense ER compartments.

Passage through Secretory Pathway—To determine the kinetics and efficiency by which RNase reached the Golgi complex, we took advantage of the observation that the secreted RNase B was Endo H-resistant (Fig. 4*C*), *i.e.* the *N*-linked glycan was converted to the complex type. Conversion occurs in the medial Golgi (25). A pulse-chase experiment showed that the first Endo H-resistant RNase B molecules appeared after 10 min chase (Fig. 4*A*). The half-time of conversion was 16 min, and the maximum level was reached after 30 min (Fig. 4*B*).

Secretion of bovine RNase molecules from the cell started after 12 min of chase (Fig. 4*E*, data not shown). The half time was 35 min, and a plateau corresponding to ~59% (± 5%) of total RNase was reached by 70 min (Fig. 4, *D* and *E*). Thus, secretion of bovine RNase was fast and relatively synchronous but inefficient. RNase A and B were secreted in about equal proportions and with identical kinetics. The lack of effect on secretion by tunicamycin, an inhibitor of *N*-linked glycosylation, confirmed that the *N*-linked glycan of RNase B was not needed for folding and had no effect on secretion (Fig. 1, *lanes 4* and *8*).

Altogether, the data indicated a rapid progression of RNase through the maturation and secretion process. For the average RNase molecule, folding was completed in 2.5 min after synthesis, transport from the rough ER to smooth membrane compartment occurred within 5 min after synthesis, glycan modification in the medial Golgi occurred after 16 min, and release from the cell occurred after 35 min. The first molecules in the pulse-labeled cohort became Endo H-resistant

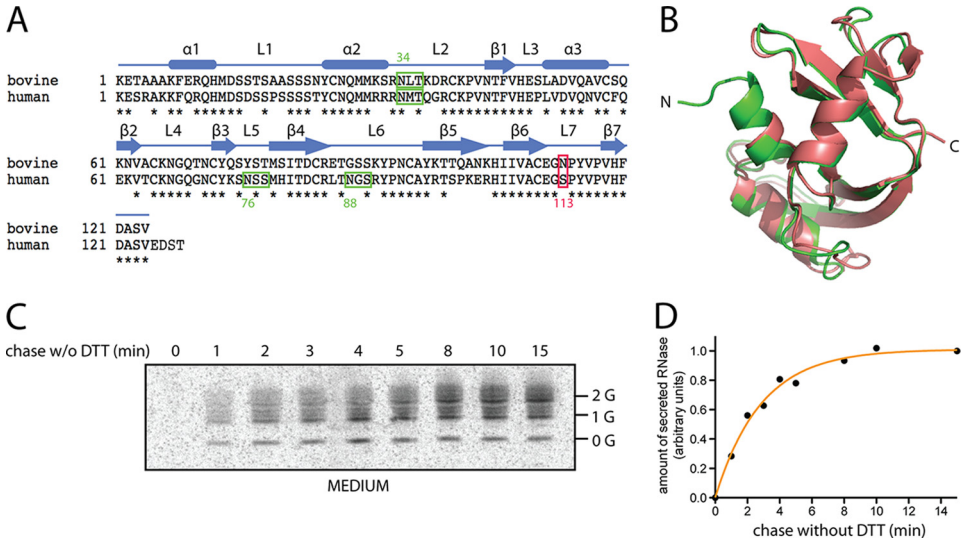

FIGURE 5. **Human RNase folds rapidly and is secreted mainly in glycosylated forms.** *A*, sequence alignment of human and bovine RNase. *Green boxes* mark the consensus sequences for *N*-linked glycosylation. Bovine RNase has one (Asn^{34}) and human three (Asn^{34}, Asn^{76}, and Asn^{88}). Note that residue 113 (*red box*) close to the C terminus is Ser in the human and Asn in the bovine RNase. Identical amino acids are marked with an *asterisk*. *B*, overlay of the crystal structures of human RNase (*red*, Protein Data Bank code 1E21) and bovine RNase (*green*, Protein Data Bank code 7RSA). *C* and *D*, DTT washout experiment with human RNase as for bovine RNase in Fig. 2 (*C* and *D*). The folding half-time was 2.5 min. *G*, glycan; *0G*, nonglycosylated; *1G*, 1 glycan; *2G*, 2 glycans; *3G*, 3 glycans.

after 10 min and already secreted after 12 min of chase. This time course was unusually rapid approaching the flow rate for a soluble bulk phase marker in the secretory pathway of CHO cells (14).

Folding and Secretion of Human RNase—Although human and bovine pancreatic RNases share 70% sequence identity and a similar structure (Fig. 5, *A* and *B*), the human enzyme differs by having three sequons for *N*-linked glycosylation instead of one (Fig. 5*A*) and by being less stable (T_m, 53 °C compared with 62 °C for bovine RNase) (7, 26).

We expressed human RNase in CHO cells and found that its maturation resembled that of the bovine counterpart in many respects. All four glycoforms (0-, 1-, 2-, and 3-glycans) were generated and secreted. With a lag time of 10–15 min, and $t_{½}$ of 27 min (Fig. 4, *D* and *E*), secretion was even faster than for bovine RNase. Also, with 73% (± 3%), the efficiency of secretion was clearly higher.

Quality Control—The final issue to be addressed was the poor efficiency of secretion of the bovine homologue. Inefficient secretion of proteins is usually due to incomplete folding and/or oligomerization (27, 28). Misfolded or unassembled proteins fail to move to the Golgi complex and beyond and are degraded by ER-associated degradation at variable rates. Frequently, they form aggregates, acquire non-native interchain disulfides, and associate permanently with chaperones.

The low efficiency of wild-type bovine RNase secretion (59% of total) was not caused by rapid degradation because after 3 h of chase, the amount of total, pulse-labeled RNase was only reduced by ~10%. Indirect immunofluorescence microscopy of RNase-expressing cells that were treated for 60 min with cycloheximide (a protein synthesis inhibitor) showed that secretion incompetent RNase was retained in the cells and resided in the ER co-localizing with calnexin (supplemental Fig. 1). When CHAPS lysates of [^{35}S]methionine- and [^{35}S]cysteine-labeled cells were analyzed by sucrose velocity gradient centrifugation, the majority of cell-associated RNase A and B were found to sediment with $S_{20,w} < 3$ consistent with monomers or small oligomers (data not shown). Thus, the cell-associated transport-incompetent RNase was not present in large, stable aggregates. SDS-PAGE after alkylation with *N*-ethylmaleimide showed that interchain disulfide bonds were not present nor did the RNase coimmunoprecipitate with BiP or calnexin, two major ER chaperones (data not shown). That the retained RNase was trypsin resistant (Fig. 2*C*) indicated that it was extensively folded.

Dimers Are Retained—To determine what was different about the retained *versus* the secreted RNase, we subjected samples of labeled CHO cell lysates and medium to size exclusion chromatography. To calibrate the column, we used purified, monomeric RNase A and B, as well as domain-swapped RNase dimers and higher oligomers prepared according to a protocol in which RNase is subjected to lyophilization from acetic acid (16). The elution profiles of monomeric RNase A and B, and RNase oligomers are shown in Fig. 6*A*. Oligomers generated in this way are predominantly composed of dimers in which the C-terminal β-strands (residues 116–124) are swapped between otherwise fully folded, oxidized, and enzymically active molecules (Fig. 7*A*) (29, 30).

When CHO cells expressing bovine RNase were pulse-labeled for 15 min, and a lysate was fractionated on the same column (Fig. 6*B*), about half of the labeled RNase was found to elute as monomers (fractions 25–28). The other half had an elution volume identical to dimers (fractions 21–23, see Fig. 6, *arrowhead*). Under the conditions used, these dimers were quite stable judging by resistance to SDS and DTT treatment before SDS-PAGE.

Interestingly, when medium samples from cells that were pulse-labeled and chased for 60 min were analyzed, the secreted RNase was exclusively in the monomeric form (Fig. 6*D*). Analysis of lysates from cells that had been pulsed for 15

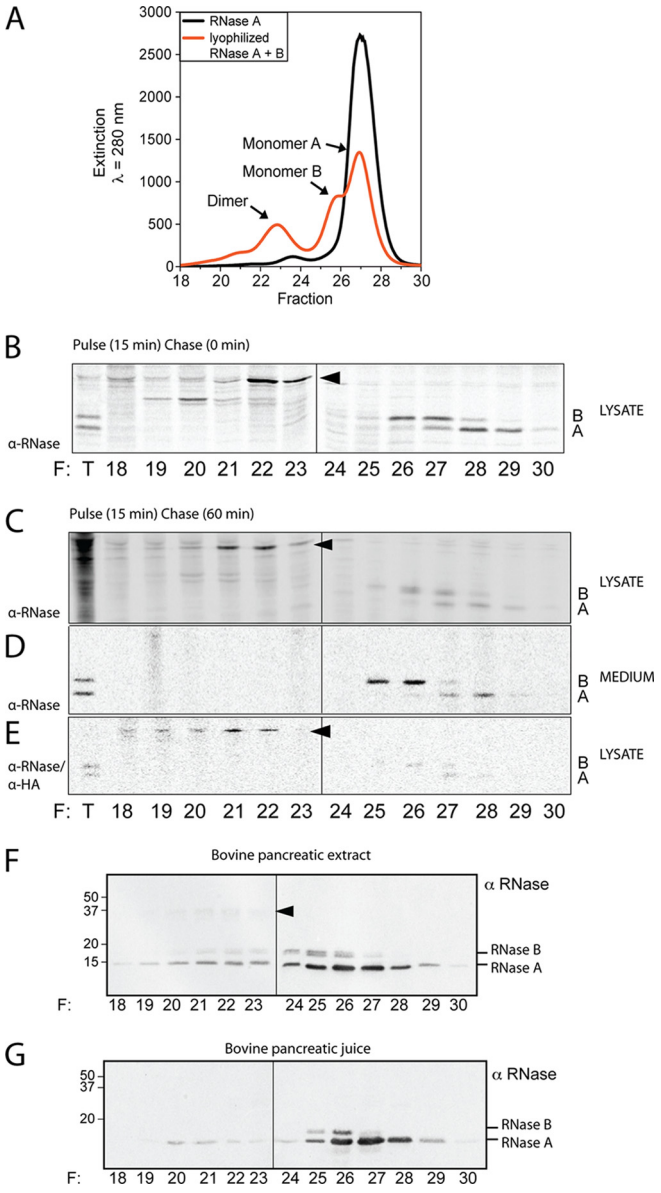

FIGURE 6. **Monomeric RNase is secreted, whereas dimers are retained.** *A*, gel filtration of RNase A monomers and domain-swapped dimers and trimers of RNase A and B. A mixture of monomers, dimers, and higher oligomers was prepared from a partially purified RNase A and B fraction by lyophilization according to the protocol by Crestfield *et al.* (16) and subjected to Superdex 75 gel filtration (*red* profile). Untreated RNase A momomers were also analyzed on the same column (*black* elution profile). Untreated RNase A peaked in fraction (*F*) 27. RNase dimers peaked in fraction 23, monomeric RNase B peaked in fraction 25, monomeric RNase A peaked in fraction 27. *B*, CHO cells expressing bovine RNase were pulsed for 15 min (0.5 mCi/ml [^{35}S]Met/Cys). After labeling, the cells were lysed. A sample of the lysate (*T*) was removed, and the rest was applied to a Superdex 75 gel filtration column. The lysate sample (*T*) and the eluted fractions were subjected to IP using polyclonal RNase antibody followed by reducing SDS-PAGE and autoradiography. The bands corresponding to dimeric RNases (*arrowheads*) were resistant to SDS and DTT. *C* and *D*, cells were pulsed for 15 min and chased for 60 min. Both media and cell lysates were fractionated on a Superdex 75 gel filtration column. Note that only the monomeric RNase was secreted. To visualize the low levels of cell-associated bovine RNase, the gels were exposed longer than in *B*. *E*, same as in *C*, but fractions were subjected to IP using polyclonal RNase antibody followed by SDS denaturation and additional IP using HA.11 antibody against the HA-tagged RNase. *F*, pancreatic tissue was homogenized in a buffer containing 2% CHAPS and fractionated on a Superdex 75 column. Fractions were subjected to IP using RNase antibodies and immunoblotted with RNase antibodies. Only few dimers were resistant to SDS and DTT (*arrowhead*). *G*, pancreatic juice was fractionated and analyzed like the tissue in *F*. *A*, RNase A; *B*, RNase B.

min and chased for additional 60 min to allow secretion-competent RNase to leave showed accumulation of dimers (Fig. 6*C*). Apparently, a large fraction of the RNase that failed to be secreted had folded into stable homodimers in the ER. To confirm that the bands detected in fractions 21–23 contained RNase, the fractions were subjected to IP with a RNase antibody. After SDS solubilization and boiling, the precipitates were reprecipitated using the HA antibody. As shown in Fig. 6*E*, the dimers were still detected.

The crystal structure of artificially generated RNase dimers shows that three hydrogen bonds are formed between Asn^{113} of both subunits in the swapped C-terminal β-strands (Fig. 7*A*) (31). The hydrogen bonding is similar to a minimal polar zipper stabilizing polyglutamine structures (32). Interestingly, the human RNase for which dimers are not observed *in vitro* (33) shares an identical C terminus with bovine RNase, except that in position 113, there is a serine. When we replaced the Asn^{113} of the bovine RNase with serine (N113S), we observed that the efficiency of secretion after a 60-min chase improved from 45% ($\pm$ 5%) to 72% ($\pm$ 5%), thus approaching the efficiency of human RNase (Fig. 7, *B* and *C*).

Indirect immunofluorescence microscopy indicated that under steady-state conditions, the cell-associated bovine RNase was mainly localized in the ER (Fig. 7*D*). Consistent with its more efficient export from the ER, human RNase seemed to be concentrated in the Golgi complex (Fig. 7*D*). Furthermore, the signal of human RNase largely disappeared after a 60-min treatment of cells with cycloheximide (data not shown). Similar to human RNase, the bovine RNase mutant N113S mainly localized in the Golgi area under steady-state conditions. To quantify the intracellular distribution of the various RNases, cells were fixed, immunostained for RNase and for the Golgi marker mannosidase II, and imaged with a wide field fluorescence microscope. The images were then analyzed to determine the relative amount of RNase signal in the Golgi and the ER regions of cells ($n > 200$) (Fig. 7*E*). The results in Fig. 7*F* confirmed that under steady-state conditions, human RNase and the bovine RNase mutant N113S were more prominent in the Golgi than wild-type bovine RNase, which was mainly present in the ER.

Taken together, our observations showed that a point mutation that weakened the domain-swapped dimers of bovine pancreatic RNase increased escape of bovine RNase from the ER, leading to a level of secretion similar to that of human RNase. The efficiency of secretion of pancreatic RNase could thus be increased by destabilizing a non-native side product of the folding process.

RNase in Bovine Pancreas—To test whether our findings in CHO cells reflected the situation in the bovine pancreas, we obtained fresh pancreatic tissue from a slaughterhouse and analyzed samples of tissue homogenate and pancreatic juice by gel filtration as above. The eluted fractions were immunoprecipitated with RNase antibody and subjected to SDS-PAGE followed by Western blotting using RNase antibody.

The tissue samples contained RNase monomers (fractions 25–28) and a small but reproducible amount of oligomers (20%). The oligomers in the pancreas were largely SDS sensitive (Fig. 6*F*, fractions 20–23). The pancreatic juice contained

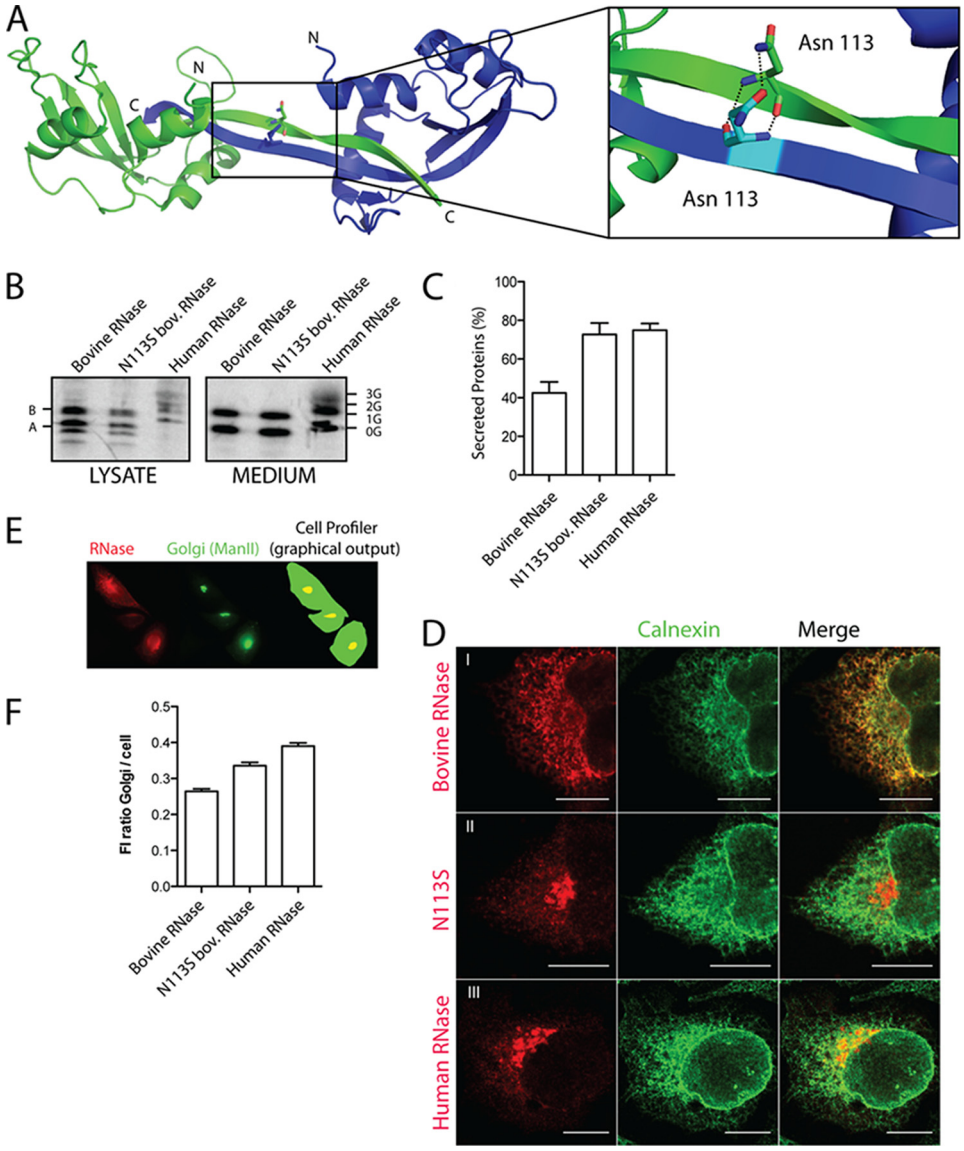

FIGURE 7. **Domain-swapped dimer.** *A*, crystal structure of the major RNase A dimer. The N and C termini are labeled. The C-terminal β-strands of the *green* and *blue* subunits are swapped. The magnification shows the two Asn^{113} that form three hydrogen bonds with each other. The figure was prepared with PyMOL. *B*, CHO cells expressing wild-type bovine RNase, N113S bovine (*bov.*) RNase, or human RNase were pulsed for 4 min (0.2 mCi/ml [^{35}S]Met/Cys) and chased for 60 min. After IP of RNase from cell lysates or medium, samples were subjected to reducing SDS-PAGE, followed by autoradiography. *C*, quantification of three independent experiments of *B*. *Bars* represent the means ± S.E. *D*, CHO cells expressing the indicated RNases were fixed and immunostained with HA and calnexin antibodies. *Scale bar* represents 10 μm. *E*, semiautomated detection of cellular outlines (*green*) and Golgi (*yellow*) with CellProfiler. *F*, ratio of fluorescence intensity (*FI*) measured from Golgi areas and cellular outlines. *Bars* represent means ± S.E. ($n > 200$ cells). *ManII*, mannosidase II; *A*, RNase A; *B*, RNase B.

almost exclusively monomers (fractions 25–28). The traces of oligomers were likely contaminants from tissue during sample extraction from the pancreas (Fig. 6*G*). Although the fraction of oligomers in the bovine pancreas was smaller than in CHO cells, the results indicated that dimers and higher oligomers were generated in pancreatic exocrine cells. As in CHO cells, the dimers failed to be efficiently secreted. Consistent with a previous report (43), only ~10–20% of the RNase in the pancreas was glycosylated.

DISCUSSION

The ER lumen provides a highly specialized environment for co- and post-translational folding and oligomeric assembly of proteins. It is filled with chaperones such as BiP, GRP94, calnexin, calreticulin, and proline isomerases, and it contains a number of different thiol oxidoreductases at high concentrations (34). These interact with nascent and full-length polypeptide chains and provide assistance in the maturation process. Folding is further affected by covalent modifications such as proteolytic cleavage and *N*-linked glycosylation. In addition, the ER possesses a quality control system that limits secretion and therefore deployment of newly synthesized proteins to those that have been correctly folded and assembled (27, 35). A selective degradation system (ER-associated degradation) is in place to handle problems arising when proteins are misfolded or fail to assemble (36).

To determine how much of a difference this folding environment makes for a specific protein, we analyzed the folding,

quality control, and secretion of pancreatic RNase in tissue culture cells. A large body of *in vitro* work has shown that RNase refolding in the absence of additional factors is slow (half-time 7 h at 25 °C and 50 h at 37 °C) (23). In contrast, when bovine RNase was expressed in CHO cells, oxidative folding was extremely rapid. Trypsin-resistant conformations were reached within 1–3 min after chain termination, and secretion-competent forms were found after 1–2 min post-translational DTT washout.

The rapid rate of folding prevented acquisition of detailed information about intermediates in the initial folding process and association with chaperones and oxidoreductases such as protein disulfide isomerase (PDI) and ERp57. The involvement of thiol oxidoreductases was likely, given that *in vitro* refolding of the RNase A and B is dramatically accelerated in the presence of these enzymes. The fastest *in vitro* refolding half-time (10 min) has been observed for RNase B in the presence of ERp57 and calnexin at 25 °C (37), *i.e.* about five times slower than in CHO cells at 37 °C. The specialized folding environment provided in the ER lumen thus caused an acceleration of folding of more than 3 orders of magnitude. In addition, it shifted the temperature optimum into the physiological range.

About half of the bovine RNase acquired a glycan in position Asn^{34}. However, the glycan had little discernable effect on the rate and efficiency of folding and secretion. A similar conclusion has been drawn from *in vitro* refolding studies with bovine RNase A and B (38). The exceptionally fast passage of the RNase from the ER to the Golgi complex and the extracellular volume was partly due to rapid folding.

Folding of bovine RNase A and B in the ER of CHO cells resulted in two major products: native monomers and dimers. Both forms were trypsin-resistant, but only the monomeric RNase passed the quality control and was secreted. Our observation that a mutation close to the C terminus (N113S) elevated the secretion efficiency of bovine RNase suggested that the majority of dimers formed in CHO cells were C-terminally domain-swapped dimers. The mutation was likely to decrease the stability of the domain-swapped dimers because the asparagines 113 form three hydrogen bonds between the connecting β-sheets that help to maintain the RNase molecules in the highly stable, dimeric state (T_m, 63 °C) (39, 40).

Analysis of bovine RNase in pancreatic exocrine cells derived from fresh bovine pancreas showed a fraction of dimers in addition to monomers (~20%). As in CHO cells, the dimers were largely retained in the cells and not secreted to the acinus. Thus, the formation of dimers as secretion-incompetent side product was not an artifact of the CHO cell system.

It has been shown that the efficiency of secretion of proteins often correlates with their thermodynamic stability (41, 42). That this rule applies to bovine RNase is suggested by the lower efficiency of secretion that we have observed for two well characterized cysteine mutants, C65S/C72S and C58S/C110S.[3] Although less stable than the bovine pancreatic RNase, the human pancreatic RNase (T_m, 54 *versus* 62 °C) was, however, more efficiently secreted (73 *versus* 59%). This suggests that the efficiency of secretion of a protein can be determined not only by the intrinsic stability of the folded, native protein, but also by additional factors such as the stability of misfolded, transport-incompetent side products. By specifically destabilizing the structure of bovine RNase dimers using a point mutation, it was, in fact, possible to increase the efficiency of secretion. The explanation for the higher efficiency of secretion of the human compared with the bovine enzyme is most likely that it does not form stable, domain-swapped dimers (33). Considering the unusual requirements and conditions in the digestive tract of a ruminant, it is possible that the exceptionally high level of stability has been a priority during the evolution of bovine pancreatic RNase. This may have been achieved at the expense of efficient folding and secretion.

Acknowledgments—We thank Dr. Marius Lemberg for providing the human RNase DNA sequence and Dr. Yoshio Misumi for providing Sec13 antiserum.

[3] R. Geiger, M. Gautschi, and A. Helenius, unpublished results.

REFERENCES

1. Braakman, I., Hoover-Litty, H., Wagner, K. R., and Helenius, A. (1991) *J. Cell Biol.* **114,** 401–411
2. Wang, N., and Hebert, D. N. (2006) *Pigment Cell Res.* **19,** 3–18
3. Kleizen, B., van Vlijmen, T., de Jonge, H. R., and Braakman, I. (2005) *Mol. Cell* **20,** 277–287
4. Anfinsen, C. B., Haber, E., Sela, M., and White, F. H., Jr. (1961) *Proc. Natl. Acad. Sci. U.S.A.* **47,** 1309–1314
5. Wedemeyer, W. J., Welker, E., Narayan, M., and Scheraga, H. A. (2000) *Biochemistry* **39,** 4207–4216
6. Raines, R. T. (1998) *Chem. Rev.* **98,** 1045–1066
7. Laity, J. H., Shimotakahara, S., and Scheraga, H. A. (1993) *Proc. Natl. Acad. Sci. U.S.A.* **90,** 615–619
8. Hammond, C., and Helenius, A. (1994) *J. Cell Biol.* **126,** 41–52
9. Hammond, C., and Helenius, A. (1994) *Science* **266,** 456–458
10. Sohda, M., Misumi, Y., Yoshimura, S., Nakamura, N., Fusano, T., Sakisaka, S., Ogata, S., Fujimoto, J., Kiyokawa, N., and Ikehara, Y. (2005) *Biochem. Biophys. Res. Commun.* **338,** 1268–1274
11. Ritter, C., Quirin, K., Kowarik, M., and Helenius, A. (2005) *EMBO J.* **24,** 1730–1738
12. Deprez, P., Gautschi, M., and Helenius, A. (2005) *Mol. Cell* **19,** 183–195
13. Mancini, R., Aebi, M., and Helenius, A. (2003) *J. Biol. Chem.* **278,** 46895–46905
14. Thor, F., Gautschi, M., Geiger, R., and Helenius, A. (2009) *Traffic* **10,** 1819–1830
15. Carpenter, A. E., Jones, T. R., Lamprecht, M. R., Clarke, C., Kang, I. H., Friman, O., Guertin, D. A., Chang, J. H., Lindquist, R. A., Moffat, J., Golland, P., and Sabatini, D. M. (2006) *Genome. Biol.* **7,** R100
16. Crestfield, A. M., Stein, W. H., and Moore, S. (1962) *Arch. Biochem. Biophys.* **1,** 217–222
17. Braakman, I., Helenius, J., and Helenius, A. (1992) *Nature* **356,** 260–262
18. Bolt, G., Kristensen, C., and Steenstrup, T. D. (2005) *Glycobiology.* **15,** 541–547
19. Allen, S., Naim, H. Y., and Bulleid, N. J. (1995) *J. Biol. Chem.* **270,** 4797–4804
20. Arnold, U., and Ulbrich-Hofmann, R. (1997) *Biochemistry* **36,** 2166–2172
21. de Silva, A., Braakman, I., and Helenius, A. (1993) *J. Cell Biol.* **120,** 647–655
22. Lodish, H. F., and Kong, N. (1993) *J. Biol. Chem.* **268,** 20598–20605

23. Shin, H. C., and Scheraga, H. A. (1999) *FEBS Lett.* **456,** 143–145
24. Fries, E., Gustafsson, L., and Peterson, P. A. (1984) *EMBO J.* **3,** 147–152
25. Kornfeld, R., and Kornfeld, S. (1985) *Annu. Rev. Biochem.* **54,** 631–664
26. Maeda, T., Mahara, K., Kitazoe, M., Futami, J., Takidani, A., Kosaka, M., Tada, H., Seno, M., and Yamada, H. (2002) *J Biochem.* **132,** 737–742
27. Ellgaard, L., and Helenius, A. (2003) *Nat. Rev. Mol. Cell Biol.* **4,** 181–191
28. Hurtley, S. M., and Helenius, A. (1989) *Annu. Rev. Cell Biol.* **5,** 277–307
29. Libonati, M., Bertoldi, M., and Sorrentino, S. (1996) *Biochem. J.* **318 (Pt 1),** 287–290
30. Park, C., and Raines, R. T. (2000) *Protein Sci.* **9,** 2026–2033
31. Liu, Y., Gotte, G., Libonati, M., and Eisenberg, D. (2001) *Nat. Struct. Biol.* **8,** 211–214
32. Perutz, M. F., Johnson, T., Suzuki, M., and Finch, J. T. (1994) *Proc. Natl. Acad. Sci. U.S.A.* **91,** 5355–5358
33. Russo, N., Antignani, A., and D'Alessio, G. (2000) *Biochemistry* **39,** 3585–3591
34. van Anken, E., and Braakman, I. (2005) *Crit. Rev. Biochem. Mol. Biol.* **40,** 191–228
35. Powers, E. T., Morimoto, R. I., Dillin, A., Kelly, J. W., and Balch, W. E. (2009) *Annu. Rev. Biochem.* **78,** 959–991
36. Vembar, S. S., and Brodsky, J. L. (2008) *Nat. Rev. Mol. Cell Biol.* **9,** 944–957
37. Zapun, A., Darby, N. J., Tessier, D. C., Michalak, M., Bergeron, J. J., and Thomas, D. Y. (1998) *J. Biol. Chem.* **273,** 6009–6012
38. Xu, G., Narayan, M., and Scheraga, H. A. (2005) *Biochemistry* **44,** 9817–9823
39. Schultz, D. A., Schmid, F. X., and Baldwin, R. L. (1992) *Protein Sci* **1,** 917–924
40. Pearce, F. G., Griffin, M. D., and Gerrard, J. A. (2009) *Biochem. Biophys. Res. Commun.* **382,** 114–118
41. Kowalski, J. M., Parekh, R. N., and Wittrup, K. D. (1998) *Biochemistry* **37,** 1264–1273
42. Wiseman, R. L., Powers, E. T., Buxbaum, J. N., Kelly, J. W., and Balch, W. E. (2007) *Cell* **131,** 809–821
43. Hirs, C. H., Moore, S., and Stein, W. H. (1953) *J. Biol. Chem.* **200,** 493–506